Inorganic Chemistry

Article

pubs.acs.org/IC

Cation−Cation Interactions in $[(UO_2)_2(OH)_n]^{4-n}$ Complexes

Samuel O. Odoh,[†] Niranjan Govind,[†] Georg Schreckenbach,[‡] and Wibe A. de Jong*[,†,§]

[†]Environmental Molecular Science Laboratory, Pacific Northwest National Laboratory, Richland, Washington 99352, United States

[‡]Department of Chemistry, University of Manitoba, Winnipeg, Manitoba, Canada R3T 2N2

Supporting Information

ABSTRACT: The structures and bonding of gas-phase $[(UO_2)_2(OH)_n]^{4-n}$ (n = 2−6) complexes have been studied using density functional theory (DFT), MP2, and CCSD(T) methods with particular emphasis on ground state structures featuring cation−cation interactions (CCIs) between the uranyl groups. An interesting trend is observed in the stabilities of members of this series of complexes. The structures of $[(UO_2)_2(OH)_2]^{2+}$, $[(UO_2)_2(OH)_4]$, and $[(UO_2)_2(OH)_6]^{2-}$ featuring CCIs are found at higher energies (by 3−27 kcal/mol) in comparison to their conventional μ_2-dihydroxo structures. In contrast, the CCI structures of $[(UO_2)_2(OH)_3]^{+}$ and $[(UO_2)_2(OH)_5]^{-}$ are respectively degenerate with and lower in energy than the structures with the μ_2-dihydroxo format. The origin of this trend lies in the symmetry-based need to balance the coordination numbers and effective atomic charges of each uranium center. The calculated IR vibrational frequencies provide signature probes that can be used in differentiating the low-energy structures and in experimentally confirming the existence of the structures featuring CCIs.

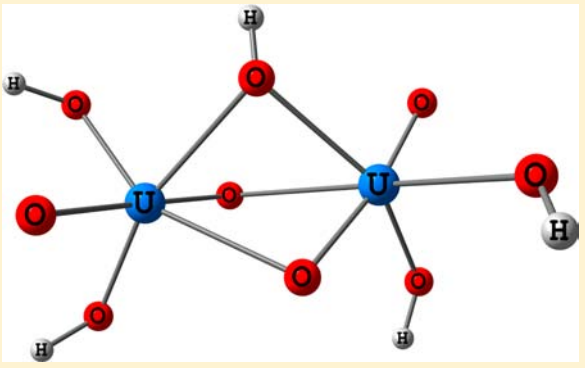

1. INTRODUCTION

There is a synergistic convergence between the application of computational approaches to the study of actinide complexes[1−24] and the resurgence of synthetic actinide chemistry. Novel actinide complexes produced via "wet" chemical synthesis are being reported regularly. A few examples of these are stable U(V) complexes[25,26] and imido-analogs of actinyl species,[27,28] among others. Complementary to these wet chemical approaches, there is a long tradition of identifying gaseous actinide compounds produced from laser-ablated solids by mass spectrometric analyses.[29−53] The transfer of actinide compounds from the solvent phase into the gaseous phase has also been demonstrated. In addition, the species produced after the laser ablation and solution-to-gas transfer processes have been reacted with other compounds (such as nebulized alcohols, water and oxygen).[34−37,40,48−50] In several cases, the products of such reactions were found to be new actinide species.

Marcalo et al. have identified multinuclear uranates with molecular formulas ranging between UO_n^- and $U_{14}O_n^-$ in their ablative work on solid uranium trioxide.[54] Anionic species, such as $U_2O_7H^-$ and $U_3O_{10}H^-$, containing hydrogen atoms were also detected in their mass spectrometric data. They noted that the hydrogen atoms were produced from water or hydroxyl groups in their samples. A recent ablation study of titanium dioxide solids resulted in the detection of similar oxy-hydroxide anions, $[(TiO_2)_x(H_2O)_yOH]^-$ and $[(TiO_2)_x(H_2O)_yO_2]^-$, after reaction with water and dioxygen.[55] The values of x and y in these species varied from 1 to 25 and 1 to 3, respectively. It can be rationalized that the previously identified uranates could also result in a similar variety of hydroxide and superoxide complexes if they are reacted with water or dioxygen.

The $[(UO_2)_2(OH)_n]^{4-n}$ series of complexes are among the possible gaseous species that can be formed on reaction of uranates with water. There is however no clear insight into the ground state molecular structures of this series of complexes. The presence of two uranyl groups in these complexes raises questions regarding the possibility of interaction between the two UO_2 groups as well as the possibility of covalent overlap between the uranium centers. Interactions between the uranyl groups fall within the general class of cation−cation interactions.[56−58] These are essentially bonding interactions in which electron density is shared between two or more cationic centers. For actinyl species, these interactions are generally propagated through bridging of two actinide centers by the axial actinyl oxo atoms. Firstly, the crystal structures of UO_3[59] and $UO_3{\cdot}H_2O$[60] are known to possess cation−cation interactions (CCIs) between neighboring uranyl groups. This is mostly due to the fact that the uranium atoms in the crystal structure have only oxo-type neighbors. As the gaseous $[(UO_2)_2(OH)_n]^{4-n}$ series of complexes could be formed through laser ablation of UO_3, it is sufficient to cautiously wonder whether structural frameworks containing these CCIs could be retained in their gas-phase structures. Secondly, the hydroxo ligand is a strong σ- and π- electron donor and its coordination in the equatorial region of the uranyl moiety generally results in an increase in the Lewis basicities of the

Received: June 17, 2013
Published: September 11, 2013

   dx.doi.org/10.1021/ic4015338 | Inorg. Chem. 2013, 52, 11269−11279

Table 1. Calculated Bond Lengths (Å) in the Lowest Energy Structures of the $[(UO_2)_2(OH)_n]^{4-n}$ Complexes Obtained at the B3LYP/TZVP Level

		μ_2-dihydroxo	μ-hydroxo-CCI	μ-hydroxo-di-CCI
dihydroxo	U−O_{yl}	1.73	1.73	1.73
	U−O_{CCI}		1.88	1.85
	pendant U−OH		1.99	2.00
	bridging U−OH	2.31	2.29	
trihydroxo	U−O_{yl}	1.77, 1.75	1.76	1.76
	U−O_{CCI}		1.82	1.84−1.86
	pendant U−OH	2.07	2.05	2.05
	bridging U−OH	2.21, 2.47	2.21, 2.43	2.30, 2.44
tetrahydroxo	U−O_{yl}	1.78	1.79	1.78
	U−O_{CCI}		1.89	1.89
	pendant U−OH	2.13	2.12	2.12
	bridging U−OH	2.37	2.34	
pentahydroxo	U−O_{yl}	1.80	1.80	1.80
	U−O_{CCI}		1.85	1.86
	pendant U−OH	2.18	2.18	2.17
	bridging U−OH	2.28, 2.56	2.27, 2.51	2.36, 2.44
hexahydroxo	U−O_{yl}	1.82	1.82	1.83
	U−O_{CCI}		1.91	1.90
	pendant U−OH	2.24	2.23	2.20
	bridging U−OH	2.42	2.39, 2.45	

uranyl oxo atoms. This increase has been found to favor the formation of CCIs between uranyl groups or with other cations.[57] It is therefore not far-fetched to also expect CCIs in the structures of the highly hydrolyzed $[(UO_2)_2(OH)_n]^{4-n}$ complexes.

In the absence of experimental data regarding the structure of $[(UO_2)_2(OH)_n]^{4-n}$ species, theoretical calculations could be carried out to resolve the interplay between the role of CCIs between the actinyl groups and the presence of hydroxide ligands. In addition, knowledge of the structural properties of the bis-uranyl complexes would provide insights into the structures and stabilities of the larger uranates (for example $U_{14}O_n^-$) and their hydroxide complexes.

While there is very little prior work on gaseous bis-uranyl hydroxide complexes, the structural and electronic properties of bis-uranyl hydroxo-aquo complexes at high pH values have been examined with experimental and theoretical approaches in aqueous solutions. In their calculations, Tsushima et al. obtained a μ_2-dihydroxo structure for $[(UO_2)_2(H_2O)_6(OH)_2]^{2+}$ complex as well as a μ-hydroxo structure for the $[(UO_2)_2(H_2O)_8(OH)]^{3+}$ complex in aqueous solution.[19] Interestingly, the μ_2-dihydroxo structure that was obtained for the aqueous $[(UO_2)_2(H_2O)_6(OH)_2]^{2+}$ complex conforms with the crystallographic work of Aberg on solid-state uranium complexes.[61] In this structure, the uranyl groups of $[(UO_2)_2(H_2O)_6(OH)_2]^{2+}$ are bridged by hydroxo ligands and their equatorial coordination spheres are satisfied by aquo ligands. Similar μ-hydroxo bridged structures have also been obtained for other actinide complexes.[62−64] On the basis of these prior works in the solid and aqueous phases,[19,61] it could be assumed that the structures of the gaseous $[(UO_2)_2(OH)_n]^{4-n}$ species would conform to the μ_2-dihydroxo structural format. It is therefore intriguing to examine the relative stabilities of this format with respect to structures featuring CCIs between the two uranyl groups. It should however be noted that the absence of first coordination sphere aquo ligands might have significant effects on the relative stabilities of gas-phase bis-uranyl species.

We report here a theoretical study of the structural features and electronic properties of the low energy structures of gaseous $[(UO_2)_2(OH)_n]^{4-n}$ complexes. Particular emphasis was given to the search of stable structures featuring CCIs between the uranyl groups in this complex. The relative energies of these CCI structures were compared to those of the more "conventional" μ_2-dihydroxo structures. The density functional theory (DFT), second order Møller−Plesset perturbation (MP2) and coupled cluster approaches were used in this work.

2. COMPUTATIONAL DETAILS

All the calculations were performed with the NWChem software suite.[65] Scalar relativistic calculations were carried out with the Stuttgart small-core effective core potential for the uranium atom.[66,67] The valence basis associated with this pseudopotential is of 10s9p5d5f3g contraction while all-electron DFT optimized valence triple-ζ polarized (TZVP) basis sets were used for the oxygen and hydrogen atoms.[68] This combination of basis set and pseudopotentials has been previously used to calculating accurate structural parameters, vibrational frequencies and reaction energies of actinide and transition metal complexes.[5,7,69−71]

The geometries of many possible structural motifs of the $[(UO_2)_2(OH)_n]^{4-n}$ (where n = 2,3,4,5 and 6) series of complexes were optimized using the hybrid B3LYP functional.[72,73] These structural motifs were obtained by rigorous examination of many possible structures without symmetry constraints. This approach allows for a sampling of the potential energy surface with the aim of detecting the lowest energy structures. Structures containing CCIs between the uranyl groups and those featuring bridging hydroxo ligands were included in this search. Structures containing equatorial aquo ligands and UO_3-type groups were also considered.

To further ascertain the relative energies of the lowest energy structures, their geometries were also optimized with the BLYP,[74,75] long-range corrected CAM-B3LYP,[76] and LC-BLYP[77] density functionals as well as the MP2[78,79] approach. The choice of these functionals varies the Hartree−Fock exchange from 0% in BLYP to 100% for long-range interactions in LC-BLYP. The correlation functional, LYP, is fixed in all the DFT approaches used in this work. Single-point calculations on the MP2-optimized geometries were carried out with the coupled cluster singles, doubles and perturbative triples, CCSD(T),[80,81] approach as well as a variety of

dx.doi.org/10.1021/ic4015338 | Inorg. Chem. 2013, 52, 11269−11279

modified density functionals: CAM-B3LYP and LC-BLYP. All electrons were correlated in the MP2 and CCSD(T) calculations. To characterize the bonding in the different structures, the Mayer–Mulliken bond orders[82,83] and natural population atomic charges were calculated at the B3LYP/TZVP level. The natural population atomic charges were obtained with the NBO program.[84,85] The zero-point vibrational energy (ZPE) corrections were included for all the reported relative energies. The ZPE corrections obtained at the MP2 level were added to the relative electronic energies obtained at the CCSD(T)//MP2 level. All the orbital maps in this work were generated with a contour value of 0.04. The calculated IR spectra were generated by using Gaussian broadening with a half-width of 12 cm^{-1}.

3. RESULTS AND DISCUSSION

3.1. Structures. The structural parameters of the three lowest energy structures of the $[(UO_2)_2(OH)_n]^{4-n}$ (n = 2–6) series of complexes obtained at the B3LYP/TZVP level are presented in Table 1. These structures are labeled as the μ_2-dihydroxo, μ-hydroxo-CCI, and di-CCI (or μ-hydroxo-di-CCI) structures, Figure 1, as they, respectively, possess two bridging hydroxo, a bridging hydroxo and a bridging CCI and two bridging CCIs between their uranyl groups. The other optimized structures of the members of this series of complexes obtained at the MP2 level of theory are presented in the Supporting Information (SI).

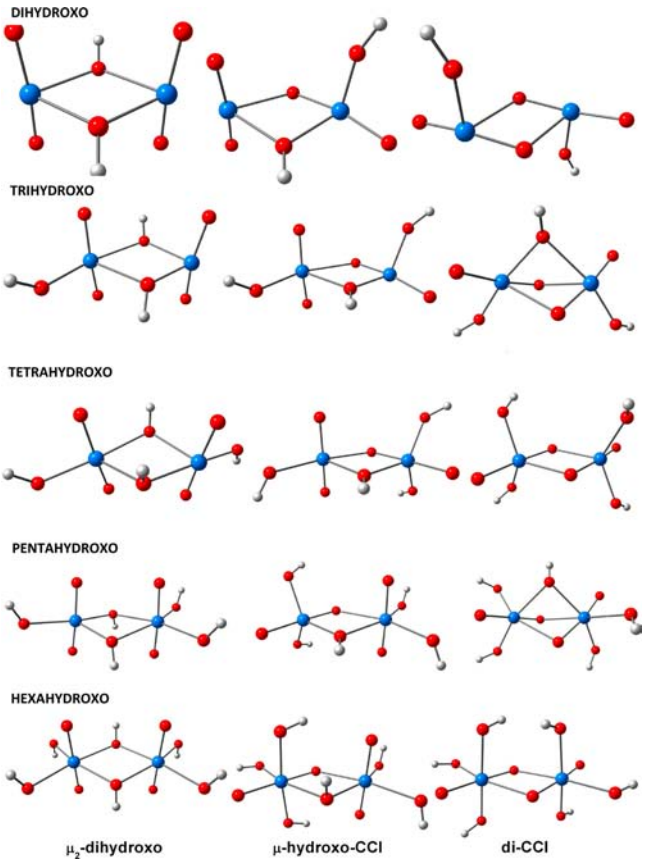

Figure 1. Low-energy structures of the bis-uranyl hydroxo complexes, $[(UO_2)_2(OH)_n]^{4-n}$. The μ_2-dihydroxo, μ-hydroxo-CCI, and di-CCI structures of the di-, tetra-, and hexahydroxo complexes are presented from left to right. The μ-hydroxo-di-CCI structure of the trihydroxo complex is shown in addition to its μ_2-dihydroxo and μ-hydroxo-CCI structures.

The U–O_{yl} and U–OH bond lengths in the μ_2-dihydroxo (two bridging hydroxo groups) structures of the $[(UO_2)_2(OH)_n]^{4-n}$ complexes are similar to those found in uranyl hydroxo species, Table S1. The bridging U–OH bonds are generally about 0.20–0.40 Å longer than the pendant U–OH bonds. This is expected given that the bridging groups are bound to two cationic uranyl centers. There is significant asymmetry in the trihydroxo and pentahydroxo complexes, with the bridging ligands being more strongly bound by one uranyl group. For example, there are two types of bridging U–OH bonds in $[(UO_2)_2(OH)_5]^-$, one set being about 2.28 Å long and the other set being about 2.56 Å in length. The calculated bond orders for the U–O_{yl} and U–OH bonds in these complexes are presented in Table 2. These are generally in good agreement with previous work on uranium hydroxo complexes, Table S1.[86−88] The U–O_{yl} bonds are essentially strong covalent double bonds with some partial triple bond characters. The U–O_{yl} and pendant U–OH bonds gradually increase in length as one progresses down the $[(UO_2)_2(OH)_n]^{4-n}$ series.[86,89−91] The increase in U–O_{yl} bond lengths down the series correlates well with a decrease in U–O_{yl} bond orders, a fact that suggests that by increasing the number of coordinated hydroxo groups, we are decreasing the covalency of the axial bonds.[86,87] The pendant U–OH bonds are mostly single bonds, with some double bond character. The bridging U–OH bonds have bond orders ranging from 0.27 to 0.93, in line with the fact that they are significantly longer than their pendant counterparts.

The general trends observed in the μ-hydroxo-CCI and μ-hydroxo-di-CCI (or simply di-CCI) structures are similar to those found in the μ_2-dihydroxo structures, Table 1. The pendant U–OH bond lengths in the μ-hydroxo-CCI structures increase from 1.99 Å in the dihydroxo complex to 2.23 Å in the hexahydroxo complex. A similar situation is found in the di-CCI structures. The U–O_{CCI} bond length (bond between uranium atom and its axial oxo atom which is involved in CCI with an adjacent uranium atom) is generally between 0.05 and 0.15 Å longer than the free U–O_{yl} bonds. This fact leads to drastic decrease in bond orders, by as much as 25%, Table 2. The U_1–O_{CCI} (between axial oxo atom of a uranyl group and an adjacent uranium atom) distances are generally between 2.30 and 2.70 Å in length. These are mostly of very weak covalent character with bond orders typically between 0.25 and 0.65, SI Tables S2–S4.

The calculated U–U distances in all these structures were generally all found to be less than the sum of the covalent radii of the uranium centers (3.92 Å), Tables S2–S4.[92] For example, the U–U distances were calculated as 3.39, 3.78, and 3.84 Å for the μ-hydroxo-di-CCI, μ-hydroxo-CCI and μ_2-dihydroxo structures of $[(UO_2)_2(OH)_5]^-$ respectively. The only exception to this is the μ_2-dihydroxo structure of the hexahydroxo complex which has a U–U distance of 3.94 Å. Compared to their μ_2-dihydroxo counterparts the U–U distances are typically shorter in the structures with CCIs. There is a contraction of the U–U distance as the degree of CCIs is increased, a fact consistent with the geometrical arrangements of the different structures. In other words, the CCI motif imposes severe structural constraints via the formation of a 4-membered ring resulting in shorter U–U distances, Figure 1. On the other hand, it is important to note that the short U–U distances, especially in the μ-hydroxo-di-CCI structures, are most likely due to the hard–hard nature of the uranium–oxygen interactions. We draw this conclusion because the calculated

dx.doi.org/10.1021/ic4015338 | Inorg. Chem. 2013, 52, 11269–11279

Table 2. Calculated Bond Orders of the Bonds in the Lowest Energy Structures of the $[(UO_2)_2(OH)_n]^{4-n}$ Complexes Obtained at the B3LYP/TZVP Level

		μ_2-dihydroxo	μ-hydroxo-CCI	μ-hydroxo-di-CCI
dihydroxo	$U-O_{yl}$	2.46	2.45	2.50
	$U-O_{CCI}$		1.77	1.92
	pendant U−OH		1.55	1.54
	bridging U−OH	0.70	0.70	
trihydroxo	$U-O_{yl}$	2.44	2.42	2.44
	$U-O_{CCI}$		2.11	1.94
	pendant U−OH	1.43	1.44	1.44
	bridging U−OH	0.93, 0.44	0.88, 0.46	0.80, 0.56
tetrahydroxo	$U-O_{yl}$	2.40	2.41	2.42
	$U-O_{CCI}$		1.79	1.85
	pendant U−OH	1.33	0.64	1.33
	bridging U−OH	0.65	1.33	
pentahydroxo	$U-O_{yl}$	2.37	2.37	2.36
	$U-O_{CCI}$		2.07	2.02
	pendant U−OH	1.22	1.26	1.25
	bridging U−OH	0.85, 0.43	0.79, 0.46	0.69, 0.58
hexahydroxo	$U-O_{yl}$	2.36	2.35	2.35
	$U-O_{CCI}$		1.82	1.89
	pendant U−OH	1.16	1.15	1.20
	bridging U−OH	0.62	0.69, 0.57	

Table 3. Relative Energies (kcal/mol) of the Low Energy Structures of $[(UO_2)_2(OH)_n]^{4-n}$, (n = 2−6) Obtained at the DFT and Ab Initio Levels

		BLYP	B3LYP	LC-BLYP	MP2	CCSD(T)//MP2
$[(UO_2)_2(OH)_2]^{2+}$	μ_2-dihydroxo	3.1	0.0	0.0	0.0	0.0
	μ-hydroxo-CCI	0.0	3.3	5.1	9.3	9.4
	di-CCI	6.7	15.5	18.7	26.2	25.7
$[(UO_2)_2(OH)_3]^{+}$	μ_2-dihydroxo	4.2	1.6	0.2	0.0	0.0
	μ-hydroxo-CCI	0.0	0.0	0.0	3.0	3.0
	μ-hydroxo-di-CCI	0.5	2.8	1.6	6.0	6.0
$[(UO_2)_2(OH)_4]$	μ_2-dihydroxo	0.4	0.0	0.0	0.0	0.0
	μ-hydroxo-CCI	0.0	2.6	4.6	8.0	5.6
	di-CCI	3.6	9.5	13.8	18.3	15.3
$[(UO_2)_2(OH)_5]^{-}$	μ_2-dihydroxo	5.2	2.4	2.1	0.4	2.3
	μ-hydroxo-CCI	2.9	0.0	1.4	1.7	1.3
	μ-hydroxo-di-CCI	0.0	0.0	0.0	0.0	0.0
$[(UO_2)_2(OH)_6]^{2-}$	μ_2-dihydroxo	0.0	0.0	0.0	0.0	0.0
	μ-hydroxo-CCI	3.0	6.1	6.5	8.8	8.1
	di-CCI	10.9	17.7	19.2	23.5	22.9

bond orders across the U−U distances are very small (0.05−0.20). This certainly suggests that direct covalent interactions between the actinide centers are essentially nonexistent. Lam et al. recently reported the synthesis and characterization of a U(V)/U(V) complex featuring a similar di-CCI motif.[93] The U−U distance in their di-CCI complex is 3.43 Å similar to that in the gas-phase μ-hydroxo-di-CCI structure of $[(UO_2)_2(OH)_5]^{-}$, 3.39 Å. Lam et al. observed longer bond lengths when di-CCI structures are bridged by sulfur, selenium or tellurium atoms.[93] The implication is that the shorter $U-O_{CCI}$ bonds (hard−hard compared to the U−S, U−Se, and U−Te) results in shorter U−U distances and is not necessarily a recipe for metal−metal covalent interactions.

3.2. Relative Energies of the μ_2-Dihydroxo and CCI Structures. The relative energies of the μ_2-dihydroxo, μ-hydroxo-CCI, and μ-hydroxo-di-CCI/di-CCI structures of the $[(UO_2)_2(OH)_n]^{4-n}$ (n = 2−6) complexes are presented in Table 3. For $[(UO_2)_2(OH)_2]^{2+}$, the μ_2-dihydroxo structure was found to be more stable than the CCI structures at the B3LYP, MP2, and CCSD(T)//MP2 levels of theory. The μ-hydroxo-CCI and di-CCI structures were found to be about 3.3 and 15.5 kcal/mol higher in energy than the μ_2-dihydroxo structure at the B3LYP/TZVP level of theory respectively. This trend is not surprising considering that one is replacing a U−OH−U bridging group in the μ_2-dihydroxo structure by a U···OU−OH group (axial $U-O_{CCI}$ bond and pendant U−OH bond) in the μ-hydroxo-CCI structure and by two O···U−OH groups (two axial $U-O_{CCI}$ bonds) in the di-CCI structure. The trend in the higher energies for the structures containing CCIs, relative to the μ_2-dihydroxo structure, is also found in $[(UO_2)_2(OH)_4]$ and $[(UO_2)_2(OH)_6]^{2-}$. In general, the MP2 and CCSD(T)//MP2 approaches give similar results and generally tend to increase the relative stabilities of the μ_2-dihydroxo structures for these complexes, Table 3.

For $[(UO_2)_2(OH)_3]^{+}$, it is found that the μ-hydroxo-CCI structure is more stable than the μ_2-dihydroxo and μ-hydroxo-

dx.doi.org/10.1021/ic4015338 | Inorg. Chem. 2013, 52, 11269−11279

di-CCI structures by about 1.6 and 2.8 kcal/mol respectively at the B3LYP/TZVP level, Table 3. The implication is that the μ_2-dihydroxo and μ-hydroxo-di-CCI structures are essentially iso-energetic and are both higher in energy than the μ-hydroxo-CCI structure. As a result of the fact that the distance between the uranium atoms are smaller than the sum of their covalent radii and the fact that several ligands are within the second coordination spheres of the actinide atoms, we used the MP2 and CCSD(T)//MP2 methods to ensure a good description of long-range effects. The CCI structures of $[(UO_2)_2(OH)_3]^+$ are within 6.0 kcal/mol of the μ_2-dihydroxo structure at the MP2 and CCSD(T)/MP2 levels, Table 3. Again, the results obtained with the CCSD(T)//MP2 approach are similar to those obtained with MP2. Although the B3LYP, LC-BLYP and CAM-B3LYP functionals, Table 3 and SI in Table S6, suggest that the μ-hydroxo-CCI structure is either iso-energetic or more stable than the μ_2-dihydroxo structure, this is inconclusive. This is because the relative energies from the MP2 and CCSD(T)// MP2 approaches favor the μ_2-dihydroxo structure, Table 3. On the whole however, it can be seen that the CCI formats, especially the di-CCI structures, are much closer in energy to the μ_2-hydroxo structure than was the case in $[(UO_2)_2(OH)_2]^{2+}$, $[(UO_2)_2(OH)_4]$, and $[(UO_2)_2(OH)_6]^{2-}$, Table 3.

The difference in the relative energy trends found between $[(UO_2)_2(OH)_3]^+$ and the n = 2, 4, and 6 $[(UO_2)_2(OH)_n]^{4-n}$ complexes correlates with the fact that the former has an odd number of hydroxo ligands in contrast to the members of the latter set that all possess even numbers of hydroxo groups. Given this, one would expect that $[(UO_2)_2(OH)_5]^-$ will be similar to the former. The relative energies presented in Table 3 show that the μ-hydroxo-CCI structure of $[(UO_2)_2(OH)_5]^-$ is iso-energetic with the μ-hydroxo-di-CCI structure and is about 2.4 kcal/mol more stable than the μ_2-dihydroxo structure when the B3LYP functional is employed. It appears that rather than just being similar to the trihydroxo complex, there is a continuation toward increased stabilities of the CCI structures. At the MP2 level, the μ_2-dihydroxo and μ-hydroxo-di-CCI structures are energetically degenerate with the μ-hydroxo-CCI structure, being about 1.7 kcal/mol higher in energy. At the CCSD(T)//MP2 levels, the μ-hydroxo-di-CCI structure is more stable than the μ_2-dihydroxo and μ-hydroxo-CCI structures by 1.3 and 2.3 kcal/mol, respectively.

To confirm the greater stability of the μ-hydroxo-di-CCI structure in $[(UO_2)_2(OH)_5]^-$, structural optimizations and vibrational frequency analyses were also carried out with the BLYP, CAM-B3LYP, and LC-BLYP functionals. In addition, single point calculations at the MP2 level were performed on geometries optimized with these density functionals. The results are presented in Table 3 and SI Table S5. All the density functionals predict the μ-hydroxo-di-CCI structure to be lower in energy than the μ_2-hydroxo structure by 1.8−5.2 kcal/mol. This agrees with the CCSD(T)//MP2 results. On the whole, the CAM-B3LYP functional is no better than the B3LYP functional, SI Table S5. This is confirmed by examining the results obtained at the B3LYP//MP2 and CAM-B3LYP//MP2 levels. The LC-BLYP functional, like all the other functionals except CAM-B3LYP, predicts the μ-hydroxo-di-CCI structure as the lowest energy structure, Table S5. In comparing the BLYP and LC-BLYP functionals, it appears that the long-range correction dampens the relative energies of the μ_2-hydroxo and μ-hydroxo-CCI structures (both within 2.1 kcal/mol compared to 5.2 kcal/mol for the BLYP functional). Single point calculations with the MP2 approach on the geometries optimized at the DFT level also indicate the μ-hydroxo-di-CCI structure to be most stable. This agrees with the CCSD(T)//MP2 and DFT results. The general conclusion from the results presented in Table 3 and SI Table S5 is that the structures of $[(UO_2)_2(OH)_5]^-$ containing CCIs are lower in energy (at nearly all levels of theory employed) than the μ_2-dihydroxo structure by between 0.4 and 5.2 kcal/mol with the μ-hydroxo-di-CCI structure being the most stable. This is a continuation of the trend toward lower relative energies for the CCI structures that commenced in $[(UO_2)_2(OH)_3]^+$, a departure from the $[(UO_2)_2(OH)_n]^{4-n}$ species with 2, 4, and 6 hydroxo ligands.

From a methodological perspective, it appears that some portion of Hartree−Fock exchange is needed for accurate description of the trends in the calculated relative energies of the bis-uranyl hydroxo species. This is especially the case for the dihydroxo (and to some extent, the tetrahydroxo) species, for which the GGA functional, BLYP, predicts a wrong trend in comparison to the hybrid DFT approaches as well as MP2 and CCSD(T)//MP2. The pure DFT functional however performs moderately well for the pentahydroxo and hexahydroxo species. This failure of BLYP for $[(UO_2)_2(OH)_2]^{2+}$ and its moderate success for $[(UO_2)_2(OH)_5]^-$ and $[(UO_2)_2(OH)_6]^{2-}$ is in line with increasing charge delocalization down the series. This is in contrast to the relatively good performance of the B3LYP, CAM-B3LYP, and LC-B3LYP functionals across the whole series. In absolute terms, the LC-BLYP functional with 100% Hartree−Fock exchange in the asymptote best mirrors the CCSD(T)//MP2 results. It is important to note that the DFT analysis changes only the exchange functional with the correlation functional (LYP) being fixed. A similar trend was also observed for PBE and its hybrid analogue, PBE0. The optimized geometries obtained with the hybrid DFT approaches are similar to those obtained with the MP2 approach. The energies obtained from single point MP2// DFT calculations are all within 0.9 kcal/mol of those obtained at the MP2 level, SI Tables S5 and S6.

3.3. CCI Structures and the Effect of Charge or Coordination Number Balance. As noted above, the μ_2-dihydroxo structures of $[(UO_2)_2(OH)_2]^{2+}$, $(UO_2)_2(OH)_4$, and $[(UO_2)_2(OH)_6]^{2-}$ are more stable than those containing CCIs. On the other hand, the μ-hydroxo-di-CCI structure is more stable than the μ_2-dihydroxo structure in $[(UO_2)_2(OH)_5]^-$. The increased stabilities of the CCI structures started with the trihydroxo complex. It would appear that the odd number of hydroxo ligands confers increased stabilization by a bridging ligand across uranyl groups linked through CCIs. Examination of Figure 1 shows that the coordination numbers of both uranium atoms (number of U−OH and strong U═O_{yl} bonds) are generally equal in the μ_2-dihydroxo structures of dihydroxo (4), tetrahydroxo (5), and hexahydroxo (6) complexes. The CCI structures of these complexes either introduce a difference between the coordination numbers of the uranium atoms or a replacement of U−OH bridges by much weaker CCI bridges, Figure 1. These two factors are associated with higher energies.

The opposite situation applies in the pentahydroxo and trihydroxo complexes. The μ_2-dihydroxo structures are now the ones associated with different uranium coordination numbers. The CCI structures on the other hand achieve some measure of coordination number balance by either replacing one bridging U−OH bond with a weaker U−O_{CCI} interaction (μ-hydroxo-CCI structures) or by replacing both bridging U−OH bonds by two weaker U−O_{CCI} interactions (μ-hydroxo-di-CCI struc-

dx.doi.org/10.1021/ic4015338 | Inorg. Chem. 2013, 52, 11269−11279

Table 4. Calculated Natural Population Atomic Charges on the Uranium and O_{yl} Atoms of Bis-uranyl Hydroxo Complexes, $[(UO_2)_2(OH)_n]^{4-n}$ (n = 2−5) Obtained at the B3LYP/TZVP Level[a]

		μ_2-dihydroxo	μ-hydroxo-CCI	μ-hydroxo-di-CCI
dihydroxo	U	2.27	2.30, 2.15	2.18
	free O_{yl}	−0.43	−0.42, −0.36	−0.45
	CCI O_{yl}		−0.65	−0.57, −0.56
trihydroxo	U	1.96, 2.10	2.00	1.98
	free O_{yl}	−0.47, −0.50	−0.49, −0.45	−0.45
	CCI O_{yl}		−0.58	−0.56
tetrahydroxo	U	1.88	1.89	1.85
	free O_{yl}	−0.53	−0.50, −0.53	−0.48
	CCI O_{yl}		−0.64	−0.63
pentahydroxo	U	1.76, 1.82	1.77, 1.83	1.74
	free O_{yl}	−0.59, −0.55	−0.58, −0.54	−0.55
	CCI O_{yl}		−0.61	−0.60

[a]di-CCI structures in the case of the dihydroxo and tetrahydroxo complexes.

tures), Figure 1. This balance of uranium coordination numbers lowers the energies of the CCI structures −5.2 to 1.4 kcal/mol relative to the μ_2-hydroxo structure in the pentahydroxo complex, Table 3. Examination of Table 4 illustrates the interplay of the uranium coordination number balance and the atomic charge balance of the uranyl units. The di-CCI structure of $[(UO_2)_2(OH)_2]^{2+}$ is symmetrical, just like the μ_2-dihydroxo structure, but the coordination numbers of the uranium atoms are lower in the former (3) than in the latter (4), Figure 1. This and the replacement of U−OH bridges by U−O_{CCI} bridges correlate well with the higher energy of the di-CCI structure, Table 3. The charges on the CCI O_{yl} atoms are larger than those obtained for the free O_{yl} groups, suggesting that the U−O_{CCI} bridges are largely electrostatic in nature. The same situation can be seen in the tetrahydroxo and hexahydroxo complexes.

The role of coordination number balance also correlates well with the calculated atomic charges. For the μ_2-dihydroxo structures of $[(UO_2)_2(OH)_3]^+$ and $[(UO_2)_2(OH)_5]^-$, there are differences between the calculated natural charges of the uranium atoms, Table 4, a result of their different equatorial coordination environments. In contrast, the CCI structures of these complexes progress toward charge balance as the number of CCIs increase. As an example, the uranium atoms of the μ-hydroxo-di-CCI structure of $[(UO_2)_2(OH)_5]^-$ have similar atomic charges, Table 4. This is achieved by enforcing similar uranium atom coordination numbers of 5, Figure 1.

The energies associated with the insertion of an hydroxide ligand into the dihydroxo and tetrahydroxo complexes can provide additional insights into the stabilization of the CCI structures of $[(UO_2)_2(OH)_3]^+$ and $[(UO_2)_2(OH)_5]^-$, respectively. For conversion of $[(UO_2)_2(OH)_4]$ to $[(UO_2)_2(OH)_5]^-$, the inserted hydroxo group is a pendant group for the μ_2-hydroxo and μ-hydroxo-CCI species but is of intra-uranyl bridging character for the di-CCI species, Figure 1. Although the insertion of the hydroxo ligand brings about some measure of charge/coordination number balance for the μ-hydroxo-CCI and di-CCI species, it is however attached between two uranyl groups in the latter. This is a recipe for additional Coulombic and orbital stabilization. The energies associated with the insertion of OH^- into the $[(UO_2)_2(OH)_4]$ species are −107.4, −112.4, and −119.3 kcal/mol for the μ_2-hydroxo, μ-hydroxo-CCI, and di-CCI, respectively, at the B3LYP/TZVP level.

3.4. Distinguishing the μ_2-Dihydroxo and CCI Structures Using Vibrational Frequencies. Given the calculated relative energies, Tables 3, any experimental attempt to ascertain the existence of CCIs in the ground state structures of the bis-uranyl complexes should be targeted at $[(UO_2)_2(OH)_5]^-$. The calculated IR spectra for the three low energy structures of $[(UO_2)_2(OH)_5]^-$ are shown in Figure 2.

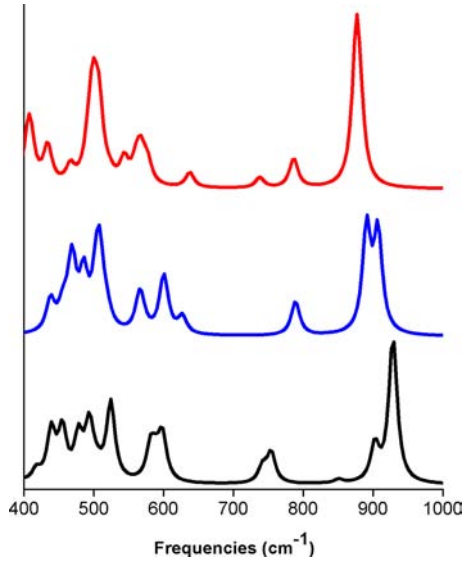

Figure 2. Calculated IR spectra for the μ_2-dihydroxo (black), μ-hydroxo-CCI (blue), and μ-hydroxo-di-CCI (red) structures of $[(UO_2)_2(OH)_5]^-$ obtained using the B3LYP functional.

There are four uranyl stretching vibrational modes between 750 and 950 cm^{-1}, Table S7. These modes can be divided into two sets between 740 and 850 and 870−930 cm^{-1}. The sets found at higher wavenumbers involve asymmetric uranyl stretching while the sets at lower wavenumbers correspond to symmetric uranyl stretching modes. The lowest uranyl stretching mode (789 cm^{-1}) in the μ-hydroxo-CCI structure and the two lowest (786 and 738 cm^{-1}) in the μ-hydroxo-di-CCI structures were predicted to yield peaks of modest IR intensities. These peaks correspond to the stretching vibrations of the U−O_{CCI} bonds. The modest intensities of these vibrational modes are in contrast to the weak IR activity of the symmetric stretching vibrations of the uranyl group in the μ_2-dihydroxo structure. This provides a tantalizing suggestion of the possibility of confirming the presence of CCIs in the ground state structure

dx.doi.org/10.1021/ic4015338 | Inorg. Chem. 2013, 52, 11269−11279

Table 5. Calculated Orbital Percentage Compositions of Two Monouranyl Species, $UO_2(OH)_2$ and $[UO_2(OH)_3]^-$ Obtained at the B3LYP/TZVP Level

		U			axial O_{yl} 2p		equatorial OH 2p		
$UO_2(OH)_2$	energy (eV)	p	d	f	1	2	1	2	3
π(d)	−10.9		14.5		32.5	32.9	7.3	7.2	
π(d)	−10.8		14.9	2.0	36.2	36.2	3.2	3.3	
σ(d)	−10.5		7.3	5.6	38.4	39.2			
π(f)	−10.2			21.7	28.0	28.3	7.3	7.6	
π(f)	−10.1			14.2	34.5	34.4	3.8	4.5	
σ(f)	−9.5	4.8	1.9	23.9	16.6	16.9	14.2	14.6	
U−OH	−9.2		7.1	1.4	4.1	3.9	38.2	37.9	
U−OH	−8.9		1.7	14.9	4.4	4.1	33.8	33.7	
U−OH	−8.6	1.2		4.0	7.4	5.9	36.6	36.8	
U−OH	−8.0	4.5	1.1	10.4	9.2	9.8	28.6	28.4	
		U			axial O_{yl} 2p		equatorial OH 2p		
$UO_2(OH)_3^-$	energy (eV)	p	d	f	1	2	1	2	3
π(d)	−5.4		12.2		35.4	26.9	4.9	4.7	7.4
π(d)	−5.2		10.5	3.7	9.2	55.7	7.2	7.0	
σ(d)	−5.7		8.8		53.31	23.31	1.0	1.1	4.2
π(f)	−4.9			18.8	14.8	48.5	2.6	2.4	5.5
π(f)	−4.8	1.0	1.2	14.2	64.8	8.6	2.4	2.5	
U−OH/σ(f)	−4.4	2.8	6.0	13.5	6.1	16.2	21.4	21.5	5.7
U−OH	−4.1		8.4		1.6	6.9	22.4	22.5	32.3
U−OH	−4.0		1.3	2.6	8.6	12.2	17.4	17.3	33.4
U−OH	−3.8			9.7			26.4	26.6	32.0
σ(f)/U−OH	−3.7	4.6	1.1	21.7	15.8	6.9	19.8	19.8	4.0
U−OH	−3.2	2.2				8.2	31.1	21.8	31.0
U−OH	−3.1	4.2		5.9	6.8	5.1	21.2	21.3	29.5

of $[(UO_2)_2(OH)_5]^-$. This is because the symmetric stretching modes of the uranyl group in the μ_2-dihydroxo structure are significantly weaker (IR) and are found at about 6−50 cm^{-1} higher wavenumbers than those in the μ-hydroxo-CCI and μ-hydroxo-di-CCI structures. A comparison of the infrared and Raman vibrational spectra might be particularly informative. At sufficiently high resolutions, the nature of the peaks around 900 cm^{-1} can also be used to distinguish the μ_2-dihydroxo from the CCI structures, Figure 2.

The peaks corresponding to wagging of the bridging hydroxo ligands at around 750 cm^{-1} for the μ_2-dihydroxo structure can also be used as probe to distinguish the μ_2-dihydroxo structure from those featuring CCIs. Overall, the calculated relative intensities of the peaks obtained with the MP2 approach confirm the usefulness of these vibrational modes, SI Figure S2.

3.5. Electronic Structures of the Bis-Uranyl Hydroxo Complexes. Regarding the electronic structures of the bis-uranyl complexes, it is important to examine whether the elongation of the U−O_{yl} and U−OH bonds occurs via the same channels as those found in their monouranyl counterparts. The orbital compositions of $UO_2(OH)_2$ and $[UO_2(OH)_3]^-$ are presented in Table 5. On average, the contributions of the axial oxo groups to the π(d), π(f) and σ(d) are similar in both of these species. However, the nature of the σ(f) and U−OH orbitals are different between these species. There is a noticeable increase in the OH contributions to the σ(f) and U−OH orbitals on going from the dihydroxo to the trihydroxo complex, Table 5. Although the U-5f contributions to these orbitals remain largely the same, the contributions from the axial oxo atoms are reduced, suggesting some competition for the 5f orbitals between the axial oxo and equatorial OH groups. This is in agreement with the findings of Ingram et al.[86] and the suggestions of Clark et al.[94] There is also an increase in the OH contributions to the σ(d) orbitals, albeit to a smaller extent than in the case of the σ(f) orbitals, Table 5.

Examination of the orbitals with predominantly σ(f) character in the μ_2-hydroxo structures of $[(UO_2)_2(OH)_2]^{2+}$ and $[(UO_2)_2(OH)_3]^+$, Figure 3, reveals the overlap between the pendant U−OH bond and a uranyl σ(f) orbital in the trihydroxo complex. This is accompanied by a decrease in the U-5f contribution to these orbitals as well as a decrease in the contributions of the bridging hydroxo groups. This competitive behavior between orbitals of the pendant and bridging hydroxo

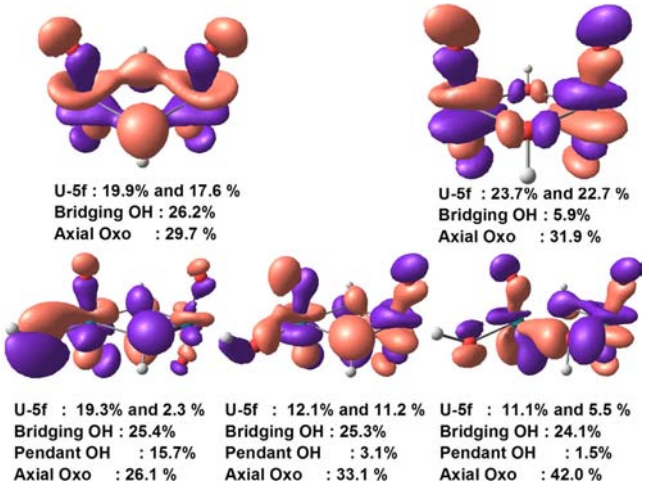

Figure 3. σ(f)/U−OH orbitals of $[(UO_2)_2(OH)_2]^{2+}$ (top) and $[(UO_2)_2(OH)_3]^+$ (bottom) and their percentage composition from various fragments.

dx.doi.org/10.1021/ic4015338 | Inorg. Chem. 2013, 52, 11269−11279

ligands is similar to the competition between the axial and hydroxo ligands found in the monouranyl complexes, Table 5.

It is also important to ascertain the origin of the general preference (with the trihydroxo and pentahydroxo species being exceptions) for structural bridging via an hydroxo ligand rather than via CCI interactions through the uranyl axial oxo atoms.[95] A natural energy decomposition analysis (NEDA[84,85]) of the $UO_2(OH)_2$ fragments in $[(UO_2)_2(OH)_4]$ was carried out at the B3LYP/TZVP level. The steric interaction energy (taken here as the sum of Coulombic interaction and Pauli repulsion energies) between the fragments were calculated as 16.6, 18.5, and 19.5 kcal/mol for the μ_2-dihydroxo, μ-hydroxo-CCI and μ-hydroxo-di-CCI structures of $[(UO_2)_2(OH)_4]$, respectively. On the other hand, the orbital (delocalization) interaction energies were calculated as −72.3, −71.6, and −62.3 kcal/mol, respectively. This implies that the preference for hydroxo bridging between the uranyl groups originates in the degree of orbital overlap between the fragments. This is because the Pauli repulsion screens the electrostatic interaction between the fragments to similar degrees in the different structures. A similar stabilization of the μ_2-dihydroxo structures as a result of orbital overlap is seen in the dihydroxo and hexahydroxo structures.

To illustrate the role of orbital overlap in stabilizing the μ_2-dihydroxo structures, some of the orbitals featuring overlap between the two $[UO_2(OH)]^+$ fragments of $[(UO_2)_2(OH)_2]^{2+}$ are presented in Figure 4. Several of the π(d), π(f), and σ(d) orbitals in the μ_2-dihydroxo structure contain significant U−OH character as a result of overlap with 2p orbitals of the bridging hydroxo groups. A similar case is obtained in the σ(f) orbitals, in which a ring-like distribution between the uranyl orbitals is formed, Figure 4. There are still overlaps between the π(d) and π(f) uranyl orbitals with atomic contributions from the bridging OH ligand and the O_{CCI} group in the μ-hydroxo-CCI structure, Figure 4. The ring-like distribution found in the σ(f) orbitals of the μ_2-dihydroxo structure are however lacking in the μ-hydroxo-CCI structure. Overlap between the $[UO_2(OH)]^+$ fragments is even smaller, limited to mainly the π(d) and σ(d) orbitals, in the μ-hydroxo-di-CCI structure, Figure 4.

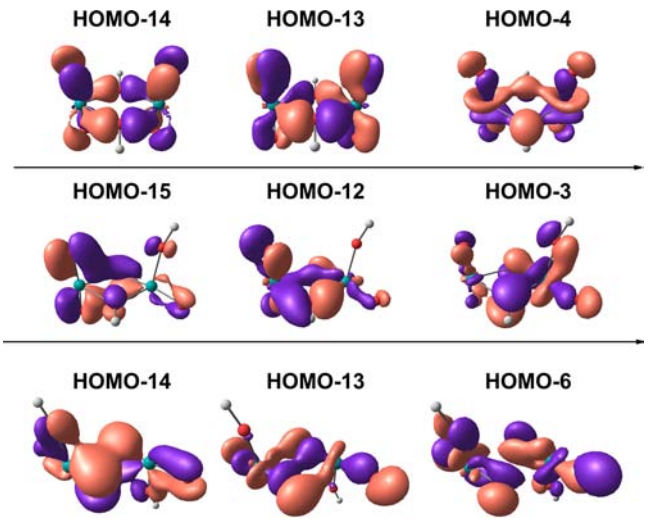

Figure 4. Some of the orbitals of the μ_2-dihydroxo (top), μ-hydroxo-CCI (middle), and μ-hydroxo-di-CCI (bottom) structures of $[(UO_2)_2(OH)_2]^{2+}$ featuring overlap between the $UO_2(OH)_2$ fragments.

3.6. Stabilities (Decomposition) of the Bis-uranyl Hydroxo Complexes. The existence (or possible observation) of the gas-phase bis-uranyl hydroxo complexes depends on several factors. Their stabilities with respect to decomposition to monouranyl hydroxide species is one of these. To this effect, we have calculated the energies associated with the decomposition reactions 1−5 at the B3LYP and CCSD(T)//MP2 levels. These energies are presented in Figure 5.

$$2[UO_2(OH)]^+ \rightarrow [(UO_2)_2(OH)_2]^{2+} \quad (1)$$

$$[UO_2(OH)]^+ + [UO_2(OH)_2] \rightarrow [(UO_2)_2(OH)_3]^+ \quad (2)$$

$$2[UO_2(OH)_2] \rightarrow [(UO_2)_2(OH)_4] \quad (3)$$

$$[UO_2(OH)_2] + [UO_2(OH)_3]^- \rightarrow [(UO_2)_2(OH)_5]^- \quad (4)$$

$$2[UO_2(OH)_3]^- \rightarrow [(UO_2)_2(OH)_6]^{2-} \quad (5)$$

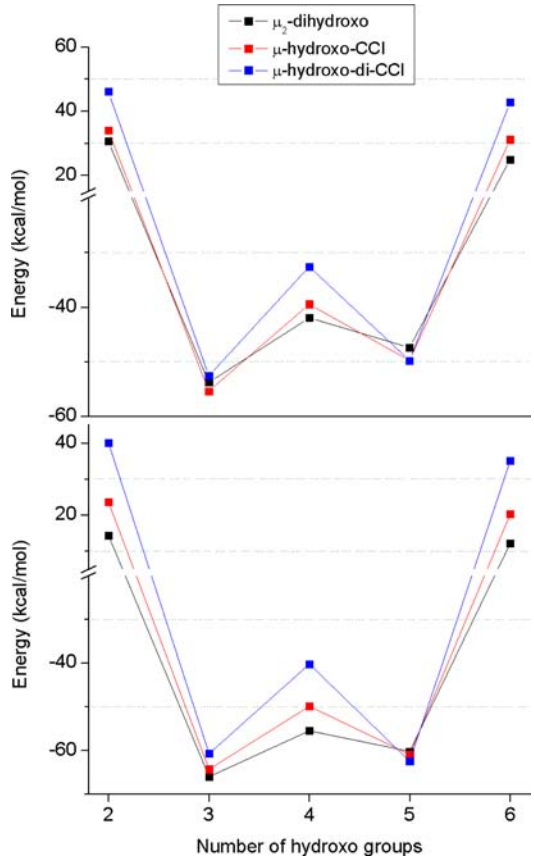

Figure 5. Calculated energies associated with the decomposition of bis-uranyl hydroxo complexes into monouranyl hydroxides obtained at the B3LYP (top) and CCSD(T)//MP2 (bottom) levels.

The decomposition of the dihydroxo and hexahydroxo bis-uranyl complexes respectively into the uranyl hydroxo and trihydroxo complexes are energetically favored, Figure 5. As such even if these species are produced during laser ablation, they would most likely be readily consumed through these decomposition channels. The endothermicities of 1 and 5 largely reflect the electrostatic and Pauli repulsions between the charged fragment species. The electrostatic interaction

dx.doi.org/10.1021/ic4015338 | Inorg. Chem. 2013, 52, 11269−11279

describes the Coulombic repulsion between the fragments whereas the Pauli interaction describes the repulsion between occupied orbitals of both fragments as they are brought closer to each other. For these complexes, the sum of electrostatic and Pauli interaction energies supersede any orbital interaction (covalency or orbital overlap) energies between the relevant fragments.

The decomposition of the bis-uranyl trihydroxo, tetrahydroxo, and pentahydroxo species into the monouranyl hydroxide species (i.e., the reverse reactions of 2, 3, and 4) is endothermic, Figure 5. Overall, the trihydroxo and pentahydroxo species appear to be most resistant to decomposition. For each bis-uranyl species, the differences between the decomposition energies obtained for its various structures reflect their relative energies, Table 3. As an example, we note that the formation energies of the di-CCI, μ-hydroxo-CCI, and μ_2-hydroxo structures of $[(UO_2)_2(OH)_4]$ from the $UO_2(OH)_2$ fragments were calculated to be −32.6, −39.5, and −42.0 kcal/mol, respectively, at the B3LYP/TZVP level and −40.2, −49.9, and −55.5 kcal/mol, respectively, at the CCSD(T)//MP2 level. The stabilities of these structures is understandable given the zero effective charge on each $UO_2(OH)_2$ fragment. This indicates that while the di-CCI structure of the tetrahydroxo complex is significantly higher in energy than the μ_2-hydroxo structure, Table 3, the CCIs can still bind the monomer units with significant amounts of energy (32.6 and 40.2 kcal/mol at the B3LYP and CCSD(T)//MP2 levels, respectively, Figure 5).

4. CONCLUSIONS

We have examined the structural and electronic properties of gas phase bis-uranyl hydroxo complexes $[(UO_2)_2(OH)_n]^{4-n}$ using a range of DFT and ab initio correlated methods. Particular emphasis was given to low energy structures featuring CCIs between the two uranyl groups.

Structurally, the progressive elongation of the $U-O_{yl}$ and U−OH bonds as the number of equatorial hydroxo ligands in the $[(UO_2)_2(OH)_n]^{4-n}$ complexes increases is similar to the case in the mononuclear uranyl complexes. A search of the low energy structures for the $[(UO_2)_2(OH)_n]^{4-n}$ complexes shows that the μ_2-dihydroxo structures are significantly more stable than those featuring CCIs for the dihydroxo, tetrahydroxo, and hexahydroxo complexes. In contrast, structures featuring uranyl CCIs were however found to be stabilized in the trihydroxo complex. This trend toward stabilization of structures with CCIs is continued in the pentahydroxo species, where the μ-hydroxo-di-CCI was found to be more stable than the μ_2-dihydroxo structure. It appears that a large portion of the increased stabilities of the CCI structures in the trihydroxo and pentahydroxo species is dictated by the degree of balance between the uranium atom coordination numbers. Structures with equal and higher uranium atom coordination numbers are generally lower in energy. A secondary factor is the distribution of pendant and bridging U−OH and $U-O_{yl}$ groups. For the bis-uranyl pentahydroxo species, the greater stability of the μ-hydroxo-di-CCI structure was confirmed at the CCSD(T)/MP2 level. Overall, our study suggests that CCIs can be induced through asymmetrical coordination (different coordination numbers) in bis-uranyl groups in the presence of strong ligands, such as the hydroxo group. The extent to which similar CCI structural arrangements have been overlooked in aqueous phase chemistry remains to be seen. Methodologically, the LC-BLYP functional with 100% Hartree−Fock exchange in the asymptote appears to best mirror the CCSD(T)//MP2 results. The degree of deficiency of the BLYP functional is related to the degree of delocalization or covalency in the bis-uranyl structure.

For the calculated structural parameters of $[(UO_2)_2(OH)_5]^-$, the U−O bonds for the oxo atoms involved in CCIs are significantly elongated in comparison to their free counterparts. This is similar to the popular case of oxo-functionalized uranyl complexes. The formation of CCIs creates discrepancies in the calculated IR vibrational frequencies associated with the stretching of the $U-O_{yl}$ bonds suggesting that the existence or otherwise of the CCI structures can be experimentally confirmed by measuring the IR spectrum of gas-phase $[(UO_2)_2(OH)_5]^-$. Examination of the bonding in $[(UO_2)_2(OH)_n]^{4-n}$ species shows that the preference for the hydroxo bridge, in contrast to bridging via the axial oxo atoms of the uranyl groups (CCI) is caused by the significant overlap between the uranyl orbitals and 2p orbitals of the hydroxo ligands.

■ ASSOCIATED CONTENT

Supporting Information

Additonal information about structures, calculated bond lengths, bond orders, vibrational frequencies, relative energies, Cartesian coordinates, and g-type functions. This material is available free of charge via the Internet at http://pubs.acs.org.

■ AUTHOR INFORMATION

Corresponding Author

*E-mail: wibe.dejong@pnnl.gov.

Present Address

[§]Lawrence Berkeley National Laboratory, Berkeley, California 94720, United States.

Notes

The authors declare no competing financial interest.

■ ACKNOWLEDGMENTS

This research was funded by the BES Heavy Element Chemistry program in the Division of Chemical Sciences, Geosciences, and Biosciences, Office of Basic Energy Sciences, U.S. Department of Energy. G.S. acknowledges financial support from the Natural Sciences and Engineering Research Council of Canada (NSERC). All calculations were performed using the Molecular Science Computing Capability in the William R. Wiley Environmental Molecular Science Laboratory, a national scientific user facility sponsored by the U.S. Department of Energy's Office of Biological and Environmental Research and located at the Pacific Northwest National Laboratory, operated for the Department of Energy by Battelle.

■ REFERENCES

(1) Barros, N.; Maynau, D.; Maron, L.; Eisenstein, O.; Zi, G. F.; Andersen, R. A. *Organometallics* **2007**, *26*, 5059.
(2) Bolvin, H.; Wahlgren, U.; Moll, H.; Reich, T.; Geipel, G.; Fanghanel, T.; Grenthe, I. *J. Phys. Chem. A* **2001**, *105*, No. 11441.
(3) Brynda, M.; Wesolowski, T. A.; Wojciechowski, K. *J. Phys. Chem. A* **2004**, *108*, 5091.
(4) Clavaguera-Sarrio, C.; Vallet, V.; Maynau, D.; Marsden, C. J. *J. Chem. Phys.* **2004**, *121*, 5312.
(5) de Jong, W. A.; Harrison, R. J.; Nichols, J. A.; Dixon, D. A. *Theor. Chem. Acc.* **2001**, *107*, 22.
(6) Gagliardi, L.; Roos, B. O. *Chem. Phys. Lett.* **2000**, *331*, 229.
(7) Groenewold, G. S.; Gianotto, A. K.; McIlwain, M. E.; Van Stipdonk, M. J.; Kullman, M.; Moore, D. T.; Polfer, N.; Oomens, J.;

Infante, I.; Visscher, L.; Siboulet, B.; De Jong, W. A. *J. Phys. Chem. A* **2008**, *112*, 508.
(8) Groenewold, G. S.; Oomens, J.; de Jong, W. A.; Gresham, G. L.; McIlwain, M. E.; Van Stipdonk, M. J. *Phys. Chem. Chem. Phys.* **2008**, *10*, 1192.
(9) Gutowski, K. E.; Cocalia, V. A.; Griffin, S. T.; Bridges, N. J.; Dixon, D. A.; Rogers, R. D. *J. Am. Chem. Soc.* **2007**, *129*, 526.
(10) Hemmingsen, L.; Amara, P.; Ansoborlo, E.; Field, M. J. *J. Phys. Chem. A* **2000**, *104*, 4095.
(11) Kozimor, S. A.; Yang, P.; Batista, E. R.; Boland, K. S.; Burns, C. J.; Clark, D. L.; Conradson, S. D.; Martin, R. L.; Wilkerson, M. P.; Wolfsberg, L. E. *J. Am. Chem. Soc.* **2009**, *131*, 12125.
(12) Nocton, G.; Horeglad, P.; Vetere, V.; Pecaut, J.; Dubois, L.; Maldivi, P.; Edelstein, N. M.; Mazzanti, M. *J. Am. Chem. Soc.* **2010**, *132*, 495.
(13) Real, F.; Vallet, V.; Marian, C.; Wahlgren, U. *J. Chem. Phys.* **2007**, 127.
(14) Schreckenbach, G.; Hay, P. J.; Martin, R. L. *Inorg. Chem.* **1998**, *37*, 4442.
(15) Schreckenbach, G.; Hay, P. J.; Martin, R. L. *J. Comput. Chem.* **1999**, *20*, 70.
(16) Schreckenbach, G.; Shamov, G. A. *Acc. Chem. Res.* **2010**, *43*, 19.
(17) Shamov, G. A.; Schreckenbach, G. *J. Am. Chem. Soc.* **2008**, *130*, 13735.
(18) Sundararajan, M.; Campbell, A. J.; Hillier, I. H. *J. Phys. Chem. A* **2008**, *112*, 4451.
(19) Tsushima, S.; Rossberg, A.; Ikeda, A.; Muller, K.; Scheinost, A. C. *Inorg. Chem.* **2007**, *46*, 10819.
(20) Vallet, V.; Wahlgren, U.; Schimmelpfennig, B.; Moll, H.; Szabo, Z.; Grenthe, I. *Inorg. Chem.* **2001**, *40*, 3516.
(21) Vazquez, J.; Bo, C.; Poblet, J. M.; de Pablo, J.; Bruno, J. *Inorg. Chem.* **2003**, *42*, 6136.
(22) Wahlin, P.; Danilo, C.; Vallet, V.; Real, F.; Flament, J. P.; Wahlgren, U. *J. Chem. Theory Comput.* **2008**, *4*, 569.
(23) Wander, M. C. F.; Kerisit, S.; Rosso, K. M.; Schoonen, M. A. A. *J. Phys. Chem. A* **2006**, *110*, 9691.
(24) Yahia, A.; Arnold, P. L.; Love, J. B.; Maron, L. *Chem. Commun.* **2009**, 2402.
(25) Arnold, P. L.; Jones, G. M.; Odoh, S. O.; Schreckenbach, G.; Magnani, N.; Love, J. B. *Nat. Chem.* **2012**, *4*, 221.
(26) Graves, C. R.; Kiplinger, J. L. *Chem. Commun.* **2009**, 3831.
(27) Hayton, T. W.; Boncella, J. M.; Scott, B. L.; Batista, E. R.; Hay, P. J. *J. Am. Chem. Soc.* **2006**, *128*, 10549.
(28) Hayton, T. W.; Boncella, J. M.; Scott, B. L.; Palmer, P. D.; Batista, E. R.; Hay, P. J. *Science* **2005**, *310*, 1941.
(29) Andrews, L.; Liang, B. Y.; Li, J.; Bursten, B. E. *Angew. Chem., Int. Ed.* **2000**, *39*, 4565.
(30) Chertihin, G. V.; Andrews, L.; Neurock, M. *J. Phys. Chem.* **1996**, *100*, 14609.
(31) Chien, W.; Anbalagan, V.; Zandler, M.; Van Stipdonk, M.; Hanna, D.; Gresham, G.; Groenewold, G. *J. Am. Soc. Mass. Spectrom.* **2004**, *15*, 777.
(32) Cornehl, H. H.; Wesendrup, R.; Diefenbach, M.; Schwarz, H. *Chem.—Eur. J.* **1997**, *3*, 1083.
(33) Di Santo, E.; Santos, M.; Michelini, M. C.; Marcalo, J.; Russo, N.; Gibson, J. K. *J. Am. Chem. Soc.* **2011**, *133*, 1955.
(34) Gibson, J. K. *Int. J. Mass Spectrom.* **2002**, *214*, 1.
(35) Gibson, J. K.; Marcalo, J. *Coord. Chem. Rev.* **2006**, *250*, 776.
(36) Gresham, G. L.; Gianotto, A. K.; Harrington, P. D.; Cao, L. B.; Scott, J. R.; Olson, J. E.; Appelhans, A. D.; Van Stipdonk, M. J.; Groenewold, G. S. *J. Phys. Chem. A* **2003**, *107*, 8530.
(37) Hunt, R. D.; Andrews, L. *J. Chem. Phys.* **1993**, *98*, 3690.
(38) Hunt, R. D.; Yustein, J. T.; Andrews, L. *J. Chem. Phys.* **1993**, *98*, 6070.
(39) Jackson, G. P.; Gibson, J. K.; Duckworth, D. C. *J. Phys. Chem. A* **2004**, *108*, 1042.
(40) Jackson, G. P.; King, F. L.; Goeringer, D. E.; Duckworth, D. C. *J. Phys. Chem. A* **2002**, *106*, 7788.
(41) Lyon, J. T.; Andrews, L.; Malmqvist, P. A.; Roos, B. O.; Yang, T. X.; Bursten, B. E. *Inorg. Chem.* **2007**, *46*, 4917.
(42) Marcalo, J.; Gibson, J. K. *J. Phys. Chem. A* **2009**, *113*, 12599.
(43) Michelini, M. D.; Marcalo, J.; Russo, N.; Gibson, J. K. *Inorg. Chem.* **2010**, *49*, 3836.
(44) Michelini, M. D.; Russo, N.; Sicilia, E. *J. Am. Chem. Soc.* **2007**, *129*, 4229.
(45) Pereira, C. C. L.; Marsden, C. J.; Marcalo, J.; Gibson, J. K. *Phys. Chem. Chem. Phys.* **2011**, *13*, 12940.
(46) Ricks, A. M.; Gagliardi, L.; Duncan, M. A. *J. Phys. Chem. Lett.* **2011**, *2*, 1662.
(47) Santos, M.; Marcalo, J.; Leal, J. P.; de Matos, A. P.; Gibson, J. K.; Haire, R. G. *Int. J. Mass Spectrom.* **2003**, *228*, 457.
(48) Van Stipdonk, M. J.; Chien, W.; Anbalagan, V.; Bulleigh, K.; Hanna, D.; Groenewold, G. S. *J. Phys. Chem. A* **2004**, *108*, 10448.
(49) Van Stipdonk, M. J.; Chien, W.; Anbalagan, V.; Gresham, G. L.; Groenewold, G. S. *Int. J. Mass Spectrom.* **2004**, *237*, 175.
(50) Van Stipdonk, M. J.; Chien, W.; Bulleigh, K.; Wu, Q.; Groenewold, G. S. *J. Phys. Chem. A* **2006**, *110*, 959.
(51) Wang, X. F.; Andrews, L.; Vlaisavljevich, B.; Gagliardi, L. *Inorg. Chem.* **2011**, *50*, 3826.
(52) Zhou, M. F.; Andrews, L.; Ismail, N.; Marsden, C. *J. Phys. Chem. A* **2000**, *104*, 5495.
(53) Zhou, M. F.; Andrews, L.; Li, J.; Bursten, B. E. *J. Am. Chem. Soc.* **1999**, *121*, 9712.
(54) Marcalo, J.; Santos, M.; de Matos, A. P.; Gibson, J. K. *Inorg. Chem.* **2009**, *48*, 5055.
(55) Barthen, N.; Millon, E.; Aubriet, F. *J. Am. Soc. Mass. Spectr.* **2011**, *22*, 508.
(56) Arnold, P. L.; Love, J. B.; Patel, D. *Coord. Chem. Rev.* **2009**, *253*, 1973.
(57) Fortier, S.; Hayton, T. W. *Coord. Chem. Rev.* **2010**, *254*, 197.
(58) Nocton, G.; Horeglad, P.; Pecaut, J.; Mazzanti, M. *J. Am. Chem. Soc.* **2008**, *130*, 16633.
(59) Siegel, S.; Hoekstra, H.; Sherry, E. *Acta Crystallogr.* **1966**, *20*, 292.
(60) Siegel, S.; Tani, B.; Viste, A.; Hoekstra, H. R. *Acta Crystallogr., B* **1972**, *B 28*, 117.
(61) Aberg, M. *Acta. Chem. Scand. A* **1978**, *32*, 101.
(62) Henry, N.; Lagrenee, M.; Loiseau, T.; Clavier, N.; Dacheux, N.; Abraham, F. *Inorg. Chem. Commun.* **2011**, *14*, 429.
(63) Thuery, P. *Acta Crystallogr. C* **2007**, *63*, M54.
(64) Thuery, P.; Masci, B. *Acta Crystallogr. C* **2002**, *58*, m556.
(65) Valiev, M.; Bylaska, E. J.; Govind, N.; Kowalski, K.; Straatsma, T. P.; Van Dam, H. J. J.; Wang, D.; Nieplocha, J.; Apra, E.; Windus, T. L.; de Jong, W. *Comput. Phys. Commun.* **2010**, *181*, 1477.
(66) Kuchle, W.; Dolg, M.; Stoll, H.; Preuss, H. *J. Chem. Phys.* **1994**, *100*, 7535.
(67) http://www.theochem.uni-stuttgart.de/pseudopotentials/clickpse.en.html (accessed July 12, 2013).
(68) Godbout, N.; Salahub, D. R.; Andzelm, J.; Wimmer, E. *Can. J. Chem.* **1992**, *70*, 560.
(69) Aubriet, F.; Gaumet, J. J.; de Jong, W. A.; Groenewold, G. S.; Gianotto, A. K.; McIlwain, M. E.; Van Stipdonk, M. J.; Leavitt, C. M. *J. Phys. Chem. A* **2009**, *113*, 6239.
(70) de Jong, W. A.; Apra, E.; Windus, T. L.; Nichols, J. A.; Harrison, R. J.; Gutowski, K. E.; Dixon, D. A. *J. Phys. Chem. A* **2005**, *109*, 11568.
(71) Groenewold, G. S.; Gianotto, A. K.; Cossel, K. C.; Van Stipdonk, M. J.; Oomens, J.; Polfer, N.; Moore, D. T.; de Jong, W. A.; McIlwain, M. E. *Phys. Chem. Chem. Phys.* **2007**, *9*, 596.
(72) Becke, A. D. *J. Chem. Phys.* **1993**, *98*, 5648.
(73) Stephens, P. J.; Devlin, F. J.; Chabalowski, C. F.; Frisch, M. J. *J. Phys. Chem.* **1994**, *98*, 11623.
(74) Becke, A. D. *Phys. Rev. A: At. Mol. Opt. Phys.* **1988**, *38*, 3098.
(75) Lee, C. T.; Yang, W. T.; Parr, R. G. *Phys. Rev. B: Condens. Matter* **1988**, *37*, 785.
(76) Yanai, T.; Tew, D. P.; Handy, N. C. *Chem. Phys. Lett.* **2004**, *393*, 51.

(77) Iikura, H.; Tsuneda, T.; Yanai, T.; Hirao, K. *J. Chem. Phys.* **2001**, *115*, 3540.
(78) Headgordon, M.; Pople, J. A.; Frisch, M. J. *Chem. Phys. Lett.* **1988**, *153*, 503.
(79) Leininger, M. L.; Allen, W. D.; Schaefer, H. F.; Sherrill, C. D. *J. Chem. Phys.* **2000**, *112*, 9213.
(80) Cizek, J. *J. Chem. Phys.* **1966**, *45*, 4256.
(81) Riley, K. E.; Pitonak, M.; Jurecka, P.; Hobza, P. *Chem. Rev.* **2010**, *110*, 5023.
(82) Bridgeman, A. J.; Cavigliasso, G.; Ireland, L. R.; Rothery, J. *J Chem. Soc., Dalton Trans.* **2001**, 2095.
(83) Mayer, I. *Chem. Phys. Lett.* **1984**, *110*, 440.
(84) Glendening, E. D.; Reed, A. E.; Carpenter, J. E.; Weinhold, F. *NBO*, version 3.1; University of Wisconsin: Madison, WI, 1987.
(85) Reed, A. E.; Curtiss, L. A.; F., W. *Chem. Rev.* **1988**, *88*, 899.
(86) Ingram, K. I. M.; Haeller, L. J. L.; Kaltsoyannis, N. *Dalton T.* **2006**, 2403.
(87) Odoh, S. O.; Walker, S. M.; Meier, M.; Stetefeld, J.; Schreckenbach, G. *Inorg. Chem.* **2011**, *50*, 3141.
(88) Wang, X. F.; Andrews, L.; Li, J. *Inorg. Chem.* **2006**, *45*, 4157.
(89) Cao, Z.; Balasubramanian, K. *J. Chem. Phys.* **2009**, *131*, No. 164504.
(90) Odoh, S. O.; Schreckenbach, G. *Inorg. Chem.* **2013**, *52*, 245.
(91) Tsushima, S. *Dalton Trans.* **2011**, *40*, 6732.
(92) Cordero, B.; Gomez, V.; Platero-Prats, A. E.; Reves, M.; Echeverria, J.; Cremades, E.; Barragan, F.; Alvarez, S. *Dalton Trans.* **2008**, 2832.
(93) Lam, O. P.; Heinemann, F. W.; Meyer, K. *Chem. Sci.* **2011**, *2*, 1538.
(94) Clark, D. L.; Conradson, S. D.; Donohoe, R. J.; Keogh, D. W.; Morris, D. E.; Palmer, P. D.; Rogers, R. D.; Tait, C. D. *Inorg. Chem.* **1999**, *38*, 1456.
(95) Comments from unknown reviewer.